Prepared for submission to JINST

Topical Workshop on Electronics for Particle Physics - TWEPP2025
6-10 October, 2025

arXiv:2511.05479v2 [cs.NE] 27 Feb 2026

FPGA-Based Real-Time Waveform Classification

I. Bekman,[a,1] **A. Aksoy,**[a] **C. Eguzo,**[a] **C. Grewing,**[a] **A. Zambanini**[a] **S. van Waasen**[a,b]

[a] *Peter Grünberg Institute - Integrated Computing Architectures (ICA | PGI-4), Forschungszentrum Jülich, 52425 Jülich, Germany*

[b] *Faculty of Engineering, Communication Systems, University of Duisburg-Essen, 47057 Duisburg, Germany*

E-mail: i.bekman@fz-juelich.de

Abstract: For self-triggered readout of SiPM sum signals, a waveform classification can aid a simple threshold trigger to reliably extract calorimetric particle hit information online at an early stage and thus reduce the volume of transmitted data. Typically, the ADC data acquisition is based on FPGAs for edge data processing. In this study, we consider look-up-table-based neural-networks and address challenges related to the re- source footprint, hardware layout, and training of binary multi-layer neural networks. We show that these structures can be trained using a genetic algorithm and achieve the inference latency compatible with dead-time free processing online.

Keywords: Online farms and online filtering, Data processing methods, Data reduction methods, Digital electronic circuits

v9

[1] Corresponding author.

Contents

1 Introduction **2**

2 Binary Neural Network **2**

2.1 Motivation for Hardware-Constrained Design 2

2.2 Network Architecture 3

2.3 HDL Conversion and Inference 3

3 Genetic Algorithm **4**

4 Results of Training **5**

5 Conclusion and Outlook **6**

1 Introduction

Particle detectors rely on sensors to record a physical event and front-end electronics to convert this event into processable data, mainly converting it into the digital domain. In this study we focus on the silicon photomultiplier (SiPM) signals digitized via analog to digital converters (ADCs). While the raw data allows a full waveform analysis and extraction of complex signal signatures, it is costly to transmit. Hence, data compression methods are required , ideally, as early as possible in the readout chain.

Data acquisition and compression is typically performed in field-programmable gate arrays (FPGAs), which allow algorithm adjustments after hardware deployment.

Artificial neural networks on hardware can offer an efficient processing of complex data. However, state-of-the-art solutions use clocked components (DSPs, BRAMs) [1, 2], leading to significant latencies.

For typical physics experiments, avoiding dead time requires specific processing speed constraints; For example a 100-sample signal window of a 12-bit ADC at 800 MSamples/s allows maximum 125 ns processing time. Therefore, the neural network (NN) implementation needs to be optimized for the FPGA hardware to achieve a lower latency. Binary neural networks (BNNs) implemented with combinatorial look-up tables (LUTs) can achieve inference latencies below 50 ns [3–6] , and, therefore, is our candidate of choice.

Our classification task identifies three categories of SiPM signal quality: "good" for expected signal shapes that can be parameterized (*e.g.* with time over threshold and amplitude); "ugly" for signals with odd shapes, for instance pile-up of two close-by events requiring the full waveform analysis; and "bad" for irrelevant noise data that can be discarded completely. The first two categories have been used for training and performance assessment of the NNs, the "bad" identifier is used for the training yet.

2 Binary Neural Network

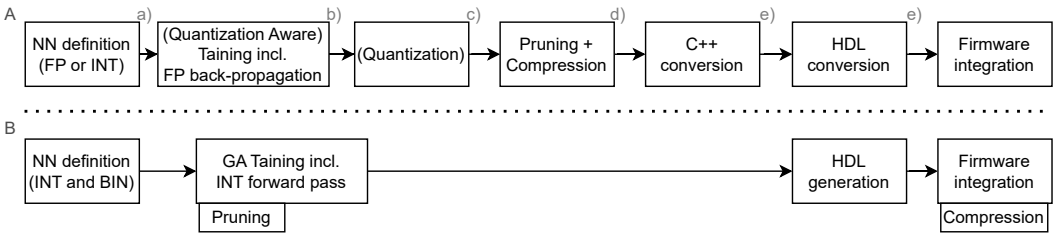

Figure 1. Comparison of implementation flow for NNs on FPGAs:
Quantization aware training (A, above) vs. Hardware-constrained learning (B, below).

2.1 Motivation for Hardware-Constrained Design

Standard FPGA neural network deployment follows this process (seen at the top of Figure 1):

(a) network definition in floating point (FP) space, including input normalization;

(b) training via iterative back-propagation with weight adjustment using loss function derivatives;

(c) quantization to map the floating point values to FPGA-compatible integers (INT8~INT16);

(d) pruning and compression removing low impact connections and nodes;

(e) encoding of the necessary Multiply-Accumulate operations in C++ and conversion to a hardware-description language via e.g. `Vitis_HLS` [7].

During inference the normalization of the input and Multiply-Accumulate operations for each neuron are expensive in terms of clock cycles and footprint (especially DSPs) on FPGAs. Moreover, step e) constraints the process to the efficiency of e.g. `Vitis_HLS` conversion.

We propose a different approach: design the network using only FPGA-appropriate operations implementable with LUT-building blocks (content-addressable memory (CAM), adders), through routing (e.g. division by 2^n i.e. bit omission), or other combinatorial logic (carry chains, multiplexers) that avoid clocked structures (as in [3]). This constraint eliminates the quantization and conversion steps but requires training suitable for non-differentiable operations.

2.2 Network Architecture

For the hidden layers we propose 2-bit neuron values and 2-bit weights. This allows multiplication operation to be replaced by a LUT-operation in a 4x4 CAM (in 2.1). First layer (2-bit) operations are constrained to 4 options listed in 2.1 in order to accommodate a 12-bit integer input and avoid the slow normalization step.

for 0..3 input						for INT input
0	0	0	0	$w = 0$	`Block`	0
0	1	2	3	$w = 1$	`Pass`	INT
1	2	3	3	$w = 2$	`Incr.`	$\min(\text{INT} \ll n, \text{MAX_INT})$
3	2	1	0	$w = 3$	`Neg.`	$\sim$ INT

(2.1)

Integer summation of N weighted inputs per neuron is performed, allowing for the sum bit width of at least $\log_2(3N)$ to prevent overflow. This step introduces, depending on the layout, a long carry chain, which is optimized in hardware by pairwise tree addition (*e.g.* $((1+2)+(3+4))$) reducing carry chain length logarithmically, helped by the lack of pipelining. The network structure is constrained to 2^n neurons per layer for efficient summation.

The `Block`ing operation (output is always 0) enables intrinsic pruning during training, see section 3.

An activation function inspired by Rectified Linear Unit (ReLU [8]) maps the integer sum back to 2-bit neuron values using three thresholds to separate the sum into four bins. The thresholds are calculated at inference time based on the number of non-zero-weights. The output is one-hot encoded, with neuron values 0 and 1 as "off" and 2 and 3 as "on".

2.3 HDL Conversion and Inference

A fixed VHDL `package` defines the implementations of functions, while a Python code takes the weights (LUT-constants) and sum threshold constants - from the results of the training - and with those generates a directly usable VHDL `entity` code. VHDL strong typing and operator overloading simplify the code.

Synthesis and implementation software can optimize across layers and neurons so that further compression of the network footprint (up to 20%) without functional changes (e.g. via LUT packing [9]) can be achieved. Optionally the VHDL attribute `KEEP` [10] can be used to keep the layers separated for ease of debugging.

3 Genetic Algorithm

Genetic algorithms (GAs) were selected for training to navigate the non-differentiable search space inherent in LUT-based binary structures.

Genetic algorithms are nature-inspired (e.g. [11, 12]) optimization methods popularized in [13] that mimic the processes behind the biological evolution.

Given a `population` of `individuals` (each representing a unique NN) with a set of `genes`, (weights) the individuals' `fitness`-es (NN accuracy) are determined and the next `generation` (iteration) is constructed by `selecting` more successful individuals, `mutating` (randomly changing few weights) and `crossing-over` (swapping sections of weights) their `genes`. Each new generation is evaluated again, and consists of more and more "fit" individuals, by construction; the loop breakout condition can be e.g. one individual reaching the target accuracy or a limit of iterations.

In this work the `deap` python package [14] is used and its `eaSimple` procedure is derived to include `elitism` (unchanged transfer of n best individuals to the next generation).

Fitness Evaluation

We simulate the SiPM signals with empiric double exponential functions for training purposes, dedicated code can be used here as well, *e.g.* [15].

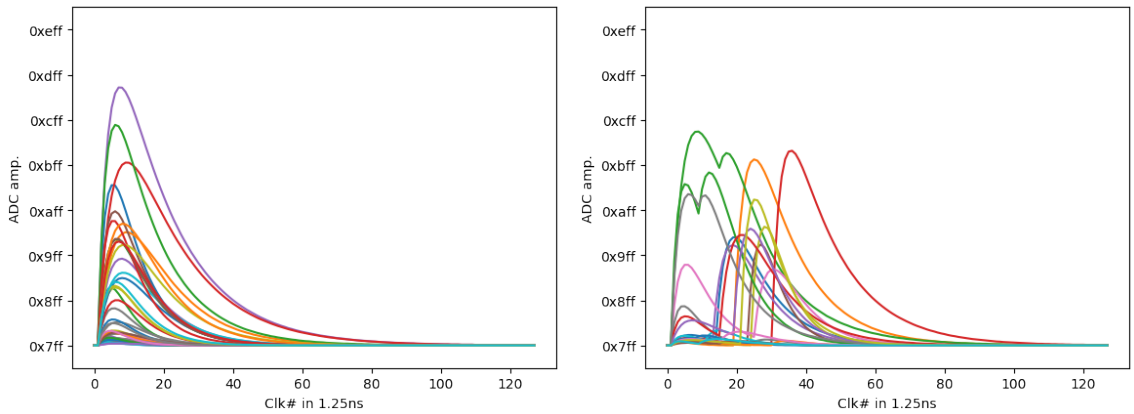

Figure 2. Simulated SiPM signal examples. Left: simple "Good"; Right: double "Ugly"

For each individual a set of "good" and "ugly" waveforms (typically 200 each) is generated. The NN predicts tuples (two binary one-hot elements) which are compared to target tuples. Since the training set is regenerated for each evaluation, fitness exhibits noisy behaviour.

Classification goodness measures how closely the predicted tuples match the target tuples, giving partial credit for partial matches (see example 3.1), and is then normalized by the tuples

length and total set size. Additionally, to avoid trivial "broken clock" classifiers achieving 50% accuracy by always predicting the same class, goodness is set to 0% whenever all predictions are identical.

$$
\begin{array}{llll}
\text{for target} = (1,0) & & & \\
(1,0) & \hat{=} & 1.0 & \\
(1,1) & \hat{=} & 0.5 & \\
(0,0) & \hat{=} & 0.5 & \\
(0,1) & \hat{=} & 0.0 &
\end{array}
\qquad
\begin{array}{llll}
\text{for MNIST target} = (0,0,0,0,0,0,0,0,0,1) & & & \\
(0,0,0,0,0,0,0,0,0,1) & \hat{=} & 10/10 & \\
(0,0,0,0,0,0,1,0,0,1) & \hat{=} & 9/10 &
\end{array}
\tag{3.1}
$$

Through the use of multi-objectives optimization in `deap` [16], we maximize the fitness and minimize the number of non-zero weights with scale 10 to 1 respectively, prioritizing accuracy while preferring "smaller" networks in the final slow improvement phase (see Figure 3).

Training is performed with typically $O(1000)$ individuals per population.

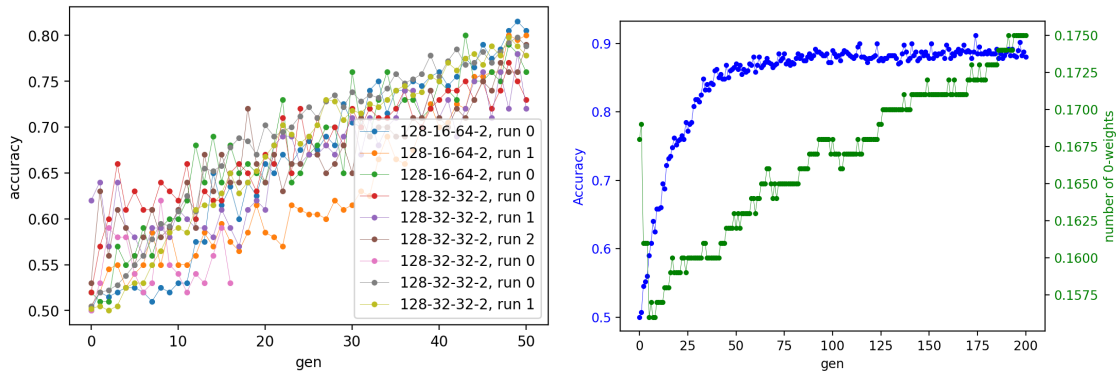

Figure 3. (left) Best accuracy progression per generation from several GA runs; (right) Best accuracy and Size (number of "0"-weights) progression per generation for one longer GA run.

4 Results of Training

We evaluate two BNN configurations. $\mathbf{BNN}_a$ with the input layer processing 128 samples (quantized from 12 bits to 7 bits), then two hidden layers 64 and 128 neurons (2-bit) respectively, and 2-bit output, can be described with the structure 128-64-128-2. The $\mathbf{BNN}_b$ has fewer neurons per hidden layer with 128-*32*-*32*-2 structure. BNN_a has a larger parameter space and so requires longer training time. Due to stochastic GA progress, it has higher risk of stalling.

As comparison baselines we implement convolutional neural networks for FINN and hls4ml converters with the same inputs and outputs, but a different internal structure: $[5,1]$ kernel and 2.0 padding and 4-6-8 hidden layers.

Table 1 summarizes the results for the target device ZCU104 [17]. Confusion matrices from a larger test set are shown in Tables 2 and 3. For BNN_a, random noise input produces neither "good" nor "ugly" classifications, indicating a robust performance.

	Accuracy in %	Latency in ns	LUTs ×k	FFs ×k	DSPs	BRAMs 18K	Training Time min * cores
FINN	74 ± 4	24850	30	20	106	5	~2 * 16
hls4ml	94.9	3050	186	112	556	120	~2 * 16
BNN_a	64 ± 5	15	58	1.5	0	0	~60 * 90
BNN_b	74 ± 5	10	23	1.5	0	0	~105 * 90

Table 1. Results and comparison of FINN 2DCNN ((128-4-6-8-2) , Kernel [5,1], padding 2.0, int8) implementation, hls4ml CNN, and BNN_a (128-64-128-2), BNN_b (128-32-32-2) with INT7 input quantization

		Predicted	
		Good	**Ugly**
True	**Good**	947	35
True	**Ugly**	410	590

		Predicted	
		Good	**Ugly**
True	**Good**	984	16
True	**Ugly**	86	914

Table 2. (Representative) confusion matrices for (left) FINN and (right) hls4ml

		Predicted		
		Good	**Ugly**	**Either**
True	**Good**	3052	1948	0
True	**Ugly**	1595	3400	5
	Either	0	0	5000

		Predicted		
		Good	**Ugly**	**Either**
True	**Good**	4883	117	0
True	**Ugly**	1533	3430	37
	Either	0	4999	1

Table 3. Confusion matrix for Good_Ugly NN (left) 128-64-128-2 and (right) 128-32-32-2

5 Conclusion and Outlook

We are addressing the processing of complex high rate data in FPGAs. Therefore, we introduce LUT-based 2-bit binary neural networks and show that they can be trained using genetic algorithms (GAs). The resulting network shows lower accuracy and time needed proportional to the network size compared to baseline approaches. However, the LUT-based approach achieves sub-20 ns latency, orders of magnitude faster than baseline methods, by using only combinatorial logic without DSPs or BRAMs. This enables real-time processing within the 125 ns constraint. New configurations of the algorithm can improve the accuracy and training time.

We provide a self-contained Python-to-VHDL NN conversion tool [18].

Several techniques are still to be investigated in order to improve the efficiency of the approach. Most prominently, frame data is typically stored in block RAM structures, which have limited port width for the retrieval. On the other hand, a typical neural network input is expecting the whole waveform to perform a classification. This creates an access bottleneck and implementing a segment-wise evaluation with several simpler networks allows for faster classifications, when a decision can be made before the the entire frame has been received.

Moreover, GAs for NNs could incorporate a gradient-based correction step to a degree into the mutation, effectively blending the exploratory power of GAs with the learning capability of gradient-based methods.

References

[1] Y. Umuroglu, N.J. Fraser, G. Gambardella, M. Blott, P. Leong, M. Jahre et al., *Finn: A framework for fast, scalable binarized neural network inference*, in *Proceedings of the 2017 ACM/SIGDA International Symposium on Field-Programmable Gate Arrays*, FPGA '17, p. 65–74, ACM, Feb., 2017, DOI.

[2] F. Fahim, B. Hawks, C. Herwig, J. Hirschauer, S. Jindariani, N. Tran et al., *hls4ml: An open-source codesign workflow to empower scientific low-power machine learning devices*, 2021.

[3] A.T.L. Bacellar, Z. Susskind, M.B. Jr, E. John, L.K. John, P.M.V. Lima et al., "Differentiable weightless neural networks." 10.48550/arXiv.2410.11112.

[4] O. Weng, M. Andronic, D. Zuberi, J. Chen, C. Geniesse, G.A. Constantinides et al., *Greater than the sum of its LUTs: Scaling up LUT-based neural networks with AmigoLUT*, in *Proceedings of the 2025 ACM/SIGDA International Symposium on Field Programmable Gate Arrays*, pp. 25–35, ACM, DOI.

[5] Y. Umuroglu, Y. Akhauri, N.J. Fraser and M. Blott, *Logicnets: Co-designed neural networks and circuits for extreme-throughput applications*, 2020.

[6] E. Wang, J.J. Davis, P.Y.K. Cheung and G.A. Constantinides, *Lutnet: Rethinking inference in fpga soft logic*, 2019.

[7] AMD Inc., *Vitis High-Level Synthesis User Guide (UG1399)*, September, 2025.

[8] A.F. Agarap, *Deep learning using rectified linear units (ReLU)*, 2019.

[9] AMD Inc., *Vivado Design Suite User Guide: Implementation (UG904)*, May, 2025.

[10] AMD Inc., *Vivado Design Suite User Guide: Synthesis (UG901)*, June, 2025.

[11] G.S. Hornby, A. Globus, D.S. Linden and J.D. Lohn, *Automated antenna design with evolutionary algorithms*, in *AIAA Space 2006*, (San Jose, CA, USA), American Institute of Aeronautics and Astronautics, September, 2006, https://ntrs.nasa.gov/citations/20060024675.

[12] M. Meloni, A. Stahl and L. Ludhova, *Optimization of a neutrino beam for the study of CP violation with the LENA and JUNO detector*, 2016.

[13] J.H. Holland, *Adaptation in Natural and Artificial Systems: An Introductory Analysis with Applications to Biology, Control, and Artificial Intelligence*, The MIT Press 10.7551/mitpress/1090.001.0001.

[14] F.-A. Fortin, F.-M. De Rainville, M.-A. Gardner, M. Parizeau and C. Gagné, *DEAP: Evolutionary algorithms made easy*, *Journal of Machine Learning Research* **13** (2012) 2171.

[15] J.P. Rodríguez, "SiPM-APD-MPPC." `https://github.com/JesusPenha/SiPM-APD-MPPC`.

[16] A. Konak, D.W. Coit and A.E. Smith, *Multi-objective optimization using genetic algorithms: A tutorial*, *Reliability Engineering & System Safety* **91** (2006) 992.

[17] "AMD zynq™ UltraScale+™ MPSoC ZCU104 evaluation kit `https://www.amd.com/en/products/adaptive-socs-and-fpgas/evaluation-boards/zcu104.html`."

[18] I. Bekman, A. Aksoy and S. Fleitmann, "HCL4BNN." `https://github.com/fzj-ica/HCL4BNN`. 10.5281/zenodo.17542690.